ELSEVIER

Three-dimensional molecular field analyses of octopaminergic agonists and antagonists for the locust neuronal octopamine receptor class 3

Akinori Hirashima,* Takumi Nagata,* Canping Pan,† Eiichi Kuwano,* Eiji Taniguchi,* and Morifusa Eto*

**Division of Bioresource and Bioenvironmental Sciences, Graduate School, Kyushu University, Fukuoka, Japan*
†Department of Applied Chemistry, Beijing Agricultural University, Beijing, People's Republic of China

The quantitative structure–activity relationship (QSAR) of a set of 70 octopaminergic agonists and 20 antagonists against octopamine receptor class 3 (OAR3) in locust nervous tissue was analyzed by molecular field analysis (MFA). MFA of these compounds evaluated effectively the energy between a probe and a molecular model at a series of points defined by a rectangular grid. Contour surfaces for the molecular fields are presented. These results provide useful information in the characterization and differentiation of octopaminergic receptor types and subtypes. © *2000 by Elsevier Science Inc.*

Keywords: Locusta migratoria, octopaminergic agonist, octopaminergic antagonist, molecular field analysis

INTRODUCTION

Octopamine (OA), which has been found to be present in high concentrations in various insect tissues, is the monohydroxylic analogue of the vertebrate hormone noradrenaline. OA receptors are perhaps the only nonpeptide receptors whose occurrence is restricted to invertebrates. OA was first discovered in the salivary glands of octopus. It has been found that OA is present in a high concentration in various invertebrate tissues.[1] This multifunctional and naturally occurring biogenic amine has been well studied and established as (1) a neurotransmitter, controlling the firefly light organ and endocrine gland activity in other insects; (2) a neurohormone, inducing mobilization of lipids and carbohydrates; (3) a neuromodulator, acting peripherally on different muscles, fat body, and sensory organs such as corpora cardiaca and the corpora allata, and (4) a centrally acting neuromodulator, influencing motor patterns, habituation, and even memory in various invertebrate species.[2,3] The action of OA is mediated through various receptor classes coupled to G proteins and is specifically linked to an adenylate cyclase. Thus, the physiological actions of OA have been shown to be associated with elevated levels of cyclic AMP.[4] Three different receptor classes, OAR1, OAR2A, and OAR2B, had been distinguished from nonneuronal tissues.[5] In the nervous system of locust *Locusta migratoria* L., a particular receptor class was characterized and established as a new class OAR3 by pharmacological investigations of the [^{3}H]OA-binding site, using various agonists and antagonists.[6–10]

Much attention has been directed at the octopaminergic system as a valid target in the development of safer and selective pesticides.[11–13] Structure–activity studies of various types of OA agonists and antagonists were also reported using the nervous tissue of the migratory locust, *L. migratoria* L.[6–10] However, information on the structural requirements of these OA agonists and antagonists for higher binding activity to OA receptor is still limited. In the process of rational drug design, it is common for the binding activity data of a set of compounds acting on a particular protein to be known, while information about the three-dimensional structure of the protein active site is absent. It is therefore of critical importance to provide information about the pharmacological properties of the types and subtypes of this OA receptor.

Our interest in octopaminergic agonists was aroused by the

The Color Plate for this article is on page 218.

Corresponding author: A. Hirashima, Division of Bioresource and Bioenvironmental Sciences, Graduate School, Kyushu University, Fukuoka 812-8581, Japan. Tel.: +81-92-642-2856; fax: +81-92-642-2864.

E-mail address: ahirasim@agr.kyushu-u.ac.jp (A. Hirashima)

Journal of Molecular Graphics and Modelling 17, 198–206, 1999

655 Avenue of the Americas, New York, NY 10010

1093-3263/99/$–see front matter
PII S1093-3263(99)00031-5

results of quantitative structure–activity relationship (QSAR) studies using various physicochemical parameters as descriptors[14,15] and a receptor surface model.[16] Furthermore, molecular modeling and conformational analysis were performed in Catalyst/Hypo to gain a better knowledge of the interactions between octopaminergic antagonists and OAR3 in order to understand the conformations required for binding activity.[17] A similar procedure was repeated using OA agonists.[18] The current work is aimed to perform 3D molecular field analysis (MFA) on a set of OA agonists and antagonists.

MOLECULAR ALIGNMENT

Multiple conformations of each molecule were generated with the Boltzmann Jump as a conformational search method. The upper limit of the number of conformations per molecule was 150. Each conformer was subjected to an energy minimization procedure to generate the lowest energy conformation for each structure. Alignment of structures through pairwise superpositioning placed all structures in the study table in the same frame of reference as the shape reference compounds, which were selected as a conformer of the most active OA agonists and antagonists, respectively. The method used for performing the alignment was the maximum common subgroup (MCSG) method. This method looks at molecules as points and lines, and uses the techniques of graph theory to identify patterns. It finds the largest subset of atoms in the shape reference compound that is shared by all the structures in the study table and uses this subset for alignment. A rigid fit of atom pairings was performed to superimpose each structure so that it overlays the shape reference compound.

GENETIC PARTIAL LEAST SQUARES

All experiments were conducted in the Cerius2 version 3.5 QSAR environment (Molecular Simulations, Burlington, MA) on a Silicon Graphics O2, running under the IRIX 6.3 operating system. Because of the large number of points used as independent variables, genetic partial least squares (G/PLS) was used to derive the QSAR models. G/PLS, a variation of genetic function approximation (GFA), can be run as an alternative to the standard GFA algorithm. G/PLS is derived from the best features of two methods: GFA and partial least squares (PLS). Both GFA and PLS have been shown to be valuable analysis tools when the data set has more descriptors than samples.

The GFA algorithm was initially conceived by taking inspiration from two seemingly disparate algorithms: Holland's genetic algorithm[19] and Friedman's[20] multivariate adaptive regression splines (MARS) algorithm. Genetic algorithms are derived from an analogy with the evolution of DNA. In this analogy, individuals are represented by a one-dimensional string of bits. An initial population of individuals is created, usually with random initial bits. A fitness function is used to estimate the quality of an individual, so that the best individuals receive the best fitness scores. Individuals with the best scores are more likely to be chosen to mate and to propagate their genetic material to offspring through the crossover operation, in which pieces of genetic material are taken from each parent and recombined to create the child. After many mating steps, the average fitness of the individuals in the population increases as good combinations of genes are discovered and spread through the population. Genetic algorithms are especially good at searching problem spaces with a large number of dimensions, as they conduct an efficiently directed sampling of the large space of possibilities. Friedman's MARS algorithm is a statistical technique for modeling data. It provides an error measure, called the lack of fit (LOF) score, that automatically penalizes models with too many features. It also inspires the use of splines as a powerful tool for nonlinear modeling. The GFA uses a genetic algorithm to perform a search over the space of possible QSAR models using the LOF score to estimate the fitness of each model. Such evolution of a population of randomly constructed models leads to the discovery of highly predictive QSARs. The GFA algorithm approach has a number of important advantages over other techniques: (1) It builds multiple models rather than a single model; (2) it automatically selects which features are to be used in the models; (3) it is better at discovering combinations of features that take advantage of correlations between multiple features; (4) it incorporates Friedman's LOF error measure, which estimates the most appropriate number of features, resists overfitting, and allows user control over the smoothness of fit; (5) it can use a larger variety of equation term types in construction of its models (for example, splines, step functions, or high-order polynomials); and (6) it provides, through study of the evolving models, additional information not available from standard regression analysis (such as the preferred model length and useful partitions of the data set).

In PLS, variables might be overlooked during interpretation or in designing the next experiment even though cumulatively they are important. This phenomenon is known as "loading spread." In GFA, equation models have a randomly chosen proper subset of the independent variables. As a result of multiple linear regression on each model, the best ones become the next generation and two of them produce an offspring. This was repeated 10 000 (default, 5 000) times. For other settings, all defaults were used. Loading spread does not occur because at most one of a set of colinear variables is retained in each model. G/PLS combines the best features of GFA and PLS.[21] Each generation has PLS applied to it instead of multiple linear regression, and so each model can have more terms in it without danger of overfitting. G/PLS retains the ease of interpretation of GFA by back-transforming the PLS components to the original variables.

MFA

QSAR modeling is an area of research pioneered by Hansch and Fujita.[22–24] QSAR attempts to model the activity of a series of compounds with measured or computed properties of the compounds. A set of 90 molecules, whose inhibitory activities were tested elsewhere using the [^{3}H]OA binding to OAR3 in the locust central nervous tissue, was selected from published data[9,10] as the target training set. The molecular structures and experimental biological activities are listed in Figures 1 and 2, and in Tables 1 and 2. Some models were statistically significant and were used to predict correctly the activities of a set of test molecules ranging over 5 orders of magnitude (maximum pK_i 9.54; minimum pK_i 3.92), indicating that these models could be useful tools to design active OA agonists and antagonists. This method generates multiple models that can be checked easily for validity. The MFA formalism calculates probe interaction energies on a rectangular grid around a bundle of active molecules. The surface is generated from a "shape

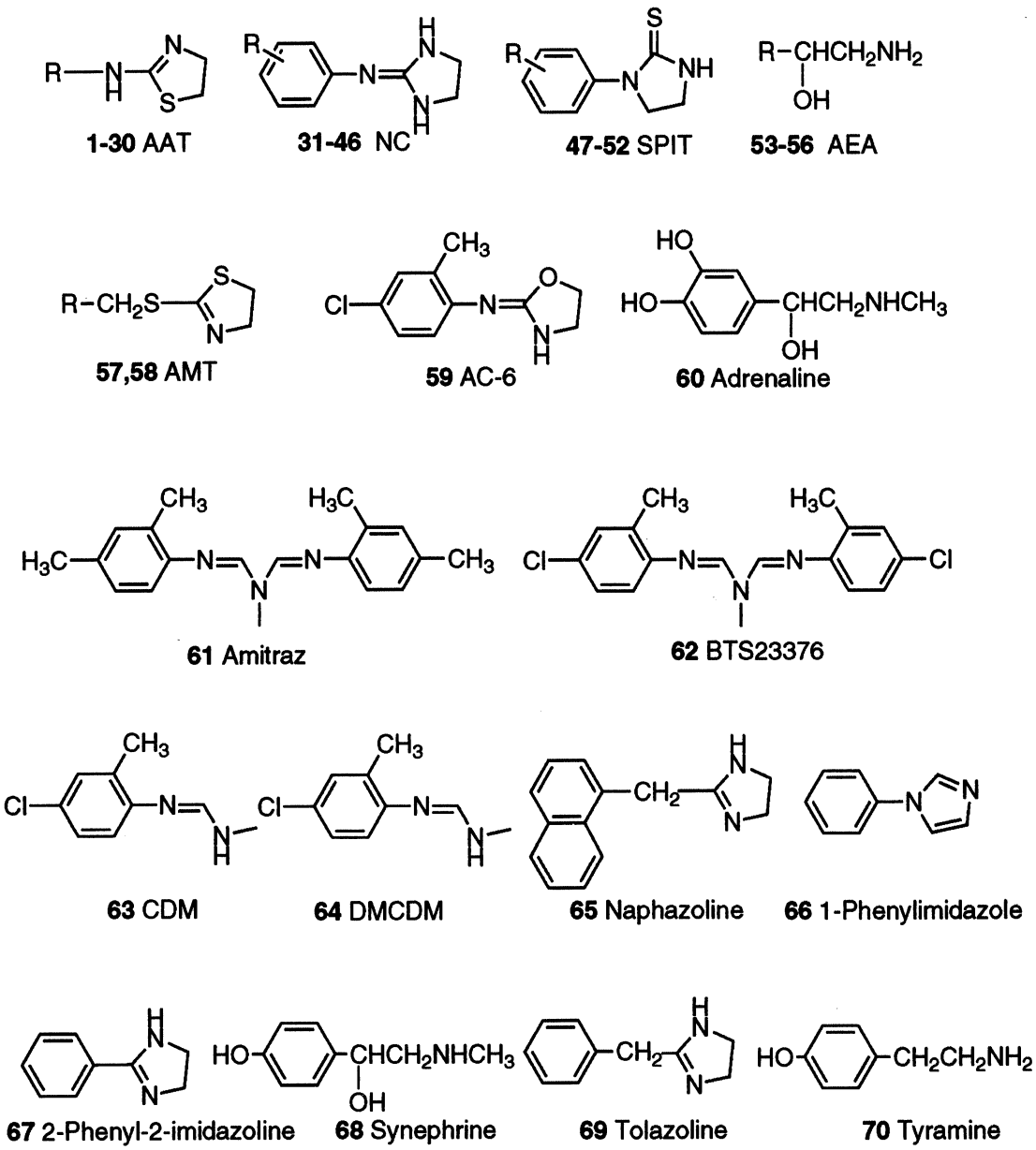

Figure 1. Structures of OA agonists used for regression analysis of study set.

field." The atomic coordinates of the contributing models are used to compute field values on each point of a 3D grid. Grid size was adjusted to 1.00 Å (default 2.00 Å). MFA evaluates the energy between a probe (H+, CH3, and Donor/Acceptor) and a molecular model at a series of points defined by a rectangular grid. Fields of molecules are represented with grids in MFA and each energy associated with an MFA grid point can serve as input for the calculation of a QSAR. These energies were added to the study table to form new columns headed according to the probe type. The numbers of variables for Eqs. (1) through (3) were 999, 891, and 1 080 for each probe, respectively. Ten percent of all new significant columns of variables were automatically used as independent X variables in the generation of QSAR.

In Eqs. (1) through (3), the descriptors *H+/x*, *H+/y*, and *H+/z* are the energies between a proton probe and the molecule at the rectangular points *x*, *y*, and *z*, respectively. The descriptors *CH3/x* and *HO-/x* are the corresponding energies of interaction for the methyl probe and Donor/Acceptor probe, respectively. To quantitatively understand the dependence of biological activities on MFA parameters of OA agonists, regression analysis was applied to representative compounds listed in Figure 1 and Table 1, leading to Equation (1).

$$pK_i = 4.64797 + 0.025515H+/338 + 0.028161H+/420 + 0.014239H+/435 - 0.028367H+/514 + 0.029638H+/832 + 0.03359CH3/445 - 0.029244CH3/528 + 0.030306CH3/556 - 0.049363CH3/637 + 0.020504CH3/732 - 0.037632HO-/121 + 0.020119HO-/419 + 0.033469HO-/428 - 0.038857HO-/741 \quad (1)$$

$n = 70$, $r^2 = 0.866$, CV-$r^2 = 0.734$, Bs-$r^2 = 0.835 \pm 0.123$

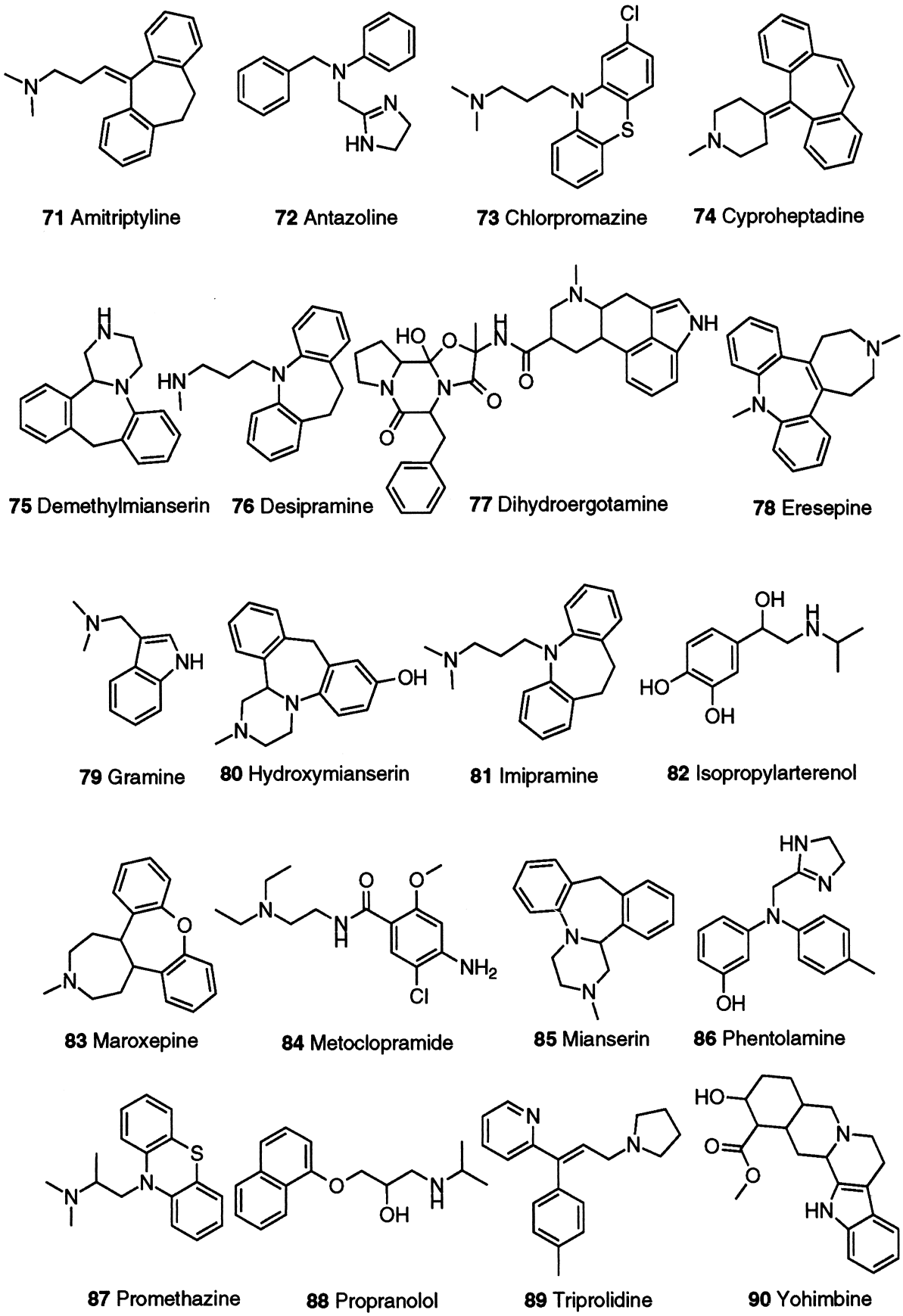

Figure 2. Structures of OA antagonists used for regression analysis of study set.

Table 1. Regression analysis of structure-OA agonist activities

Compound			pK_i		
No.	R	K_i (nM)	Observed	Calculated[a]	Deviation
1	AAT $PhCH_2$	280 ± 59[b]	6.55	6.83	−0.28
2	AAT 2-Cl-$PhCH_2$	440 ± 189[b]	6.36	6.32	0.04
3	AAT 2-F-$PhCH_2$	447 ± 125[b]	6.35	6.79	−0.44
4	AAT 2-CH_3-$PhCH_2$	650 ± 360[b]	6.19	4.80	1.39
5	AAT 2-CF_3-$PhCH_2$	290 ± 203[b]	6.54	6.80	−0.26
6	AAT 3-Cl-$PhCH_2$	95 ± 66[b]	7.02	7.46	−0.44
7	AAT 3-F-$PhCH_2$	250 ± 75[b]	6.60	7.52	−0.92
8	AAT 3-CH_3-$PhCH_2$	34 ± 26[b]	7.47	7.46	0.01
9	AAT 3-CF_3-$PhCH_2$	380 ± 266[b]	6.42	6.78	−0.36
10	AAT 3-NO_2-$PhCH_2$	185 ± 33[b]	6.73	6.01	0.72
11	AAT 4-Cl-$PhCH_2$	89 ± 6[b]	7.05	6.70	0.35
12	AAT 4-F-$PhCH_2$	460 ± 124[b]	6.34	6.73	−0.39
13	AAT 4-CH_3-$PhCH_2$	38 ± 16[b]	7.42	7.42	0
14	AAT 4-OCH_3-$PhCH_2$	9 ± 6.3[b]	8.05	7.64	0.41
15	AAT 2,3-Cl_2-$PhCH_2$	42 ± 19[b]	7.38	7.01	0.37
16	AAT 2,4-Cl_2-$PhCH_2$	1.7 ± 1.1[b]	8.77	7.77	1.00
17	AAT 2-Cl,4-F-$PhCH_2$	184 ± 90[b]	6.74	7.78	−1.04
18	AAT 2,5-Cl_2-$PhCH_2$	132 ± 83[b]	6.88	7.17	−0.29
19	AAT 2,6-Cl_2-$PhCH_2$	1 270 ± 635[b]	5.90	6.27	−0.37
20	AAT 3,4-Cl_2-$PhCH_2$	14 ± 4.2[b]	7.85	7.43	0.42
21	AAT 3-Cl,4-F-$PhCH_2$	109 ± 59[b]	6.96	6.57	0.39
22	AAT 3,4-F_2-$PhCH_2$	445 ± 196[b]	6.35	6.62	−0.27
23	AAT 3,5-Cl_2-$PhCH_2$	1[b]	9.00	8.31	0.69
24	AAT $PhCH_3CH$ (L)	37 ± 23[b]	7.43	6.87	0.56
25	AAT $PhCH_3CH$ (D)	5 000 ± 2 600[b]	5.30	5.84	−0.54
26	AAT $PhCH_2CH_2$	5 500 ± 1 920[b]	5.26	5.82	−0.56
27	AAT 4-Cl-$PhCH_2CH_2$	264 ± 95[b]	6.58	6.31	−0.27
28	AAT 3-Pyridyl-CH_2	8 330 ± 2 500[b]	5.08	5.13	−0.05
29	AAT 1-Morpholino$(CH_2)_2$	70 800 ± 19 000[b]	4.15	4.38	−0.23
30	AAT 1-Morpholino$(CH_2)_3$	121 000 ± 31 400[b]	3.92	3.98	−0.06
31	NC H	23 ± 5[c]	7.63	7.50	0.13
32	NC 4-Br	15 ± 3[c]	7.83	8.52	−0.69
33	NC 2,4-Cl_2	0.81 ± 0.18[c]	9.09	8.54	0.55
34	NC 2-CH3,4-Cl	0.87 ± 0.32[c]	9.06	9.39	−0.33
35	NC 2,4-$(CH_3)_2$	1.02 ± 0.42[c]	8.99	8.24	0.75
36	NC 2,6-Cl_2	47 ± 18[c]	7.32	7.02	0.30
37	NC 2,6-$(CH_3)_2$	20 ± 7[c]	7.70	7.80	−0.10
38	NC 2,6-$(CH_2CH_3)_2$	0.3 ± 0.4[c]	9.54	9.02	0.52
39	NC 2,6-$[CH(CH_3)_2]_2$	132 ± 35.6[c]	6.88	7.49	−0.61
40	NC 2,4,5-Cl_3	2.27 ± 0.89[c]	8.64	8.87	−0.23
41	NC 2,4,6-Cl_3	19 ± 3[c]	7.73	7.78	−0.05
42	NC 2,6-Cl_2,4-NH_2	58 ± 16[c]	7.24	7.01	0.23
43	NC 2,6-Cl_2,4-N_3	44.5 ± 7.1[c]	7.35	7.41	−0.06
44	NC 2,4,6-$(CH_3)_3$	4.38 ± 1.30[c]	8.36	9.03	−0.67
45	NC 2,4,6-$(CH_2CH_3)_3$	0.56 ± 0.14[c]	9.25	8.43	0.82
46	NC 2,6-$(CH_2CH_3)_2$,4-N_3	1.05 ± 0.47[c]	8.98	9.09	−0.11
47	SPIT 4-Cl	280 ± 134[b]	6.55	6.37	0.18
48	SPIT 2,3-Cl_2	37 100 ± 7 770[b]	4.43	5.02	−0.59
49	SPIT 2-CH_3,4-Cl	20 ± 9[b]	7.70	7.56	0.14
50	SPIT 2,4-$(CH_3)_2$	1 660 ± 700[b]	5.78	6.58	−0.80
51	SPIT 2,6-$(CH_2CH_3)_2$	170 ± 51[b]	6.77	7.14	−0.37
52	SPIT 2,4,5-Cl_3-$PhCH_2$	1 040 ± 730[b]	5.98	5.58	0.40
53	AEA Ph (DL)	115 ± 39[c]	6.94	6.94	0

Table 1. (Continued)

Compound			pK_i		
No.	R	K_i (nM)	Observed	Calculated[a]	Deviation
54	AEA 3-OH-Ph	5 050 ± 1 860[c]	5.30	5.47	−0.17
55	AEA 4-OH-Ph	7.9 ± 0.9[c]	8.18	7.91	0.27
56	AEA 3,4-$(OH)_2$-Ph	475 ± 42[c]	6.32	6.53	−0.21
57	AMT $PhCH_2$	760 ± 243[b]	6.12	6.39	−0.27
58	AMT 4-Cl-PhCO	17 500 ± 3 670[b]	4.76	5.29	−0.53
59	AC-6	0.95 ± 0.24[c]	9.02	9.09	−0.07
60	Adrenaline	416 ± 75[c]	6.38	6.46	−0.08
61	Amitraz	22 ± 5[c]	7.67	8.04	−0.37
62	BTS23376	8.9 ± 0.6[c]	8.05	7.48	0.57
63	CDM	137 ± 70[c]	6.91	7.37	−0.46
64	DMCDM	1.97 ± 0.76[c]	8.74	8.89	−0.15
65	Naphazoline	3.03 ± 2.61[c]	8.52	8.09	0.43
66	Phenylimidazole	813 ± 561[c]	6.09	5.76	0.33
67	2-Phenyl-2-imidazolidine	16 200 ± 4 700[c]	4.79	4.32	0.47
68	Synephrine	3.38 ± 0.64[c]	8.47	7.92	0.55
69	Tolazoline	18.5 ± 16[c]	7.73	7.84	−0.11
70	Tyramine	51.6 ± 17.5[c]	7.29	7.04	0.25

[a] Calculated by Eq. (1).
[b] Personal communication (T. Roeder, Hamburg University, Germany).
[c] Cited from Roeder.[9]

The term *n* means the number of data points; r^2 is the square of the correlation coefficient, which is used to describe the goodness of fit of the data in the study table to the QSAR model; cross-validated r^2 (CV-r^2) is a squared correlation coefficient generated during a validation procedure using the equation: CV-r^2 = (SD − PRESS)/SD; SD is the sum of squared deviations of the dependent variable values from their mean; the predicted sum of squares (PRESS) is the sum of overall compounds of the squared differences between the actual and the predicted values for the dependent variables. The PRESS value is computed during a validation procedure for the entire training set. The larger the PRESS value, the more reliable is the equation. A CV-r^2 is usually smaller than the overall r^2 for a QSAR equation. It is used as a diagnostic tool to evaluate the predictive power of an equation generated by the PLS method. Cross-validation is often used to determine how large a model (number of terms) can be used for a given data set. For instance, the number of components retained in PLS can be selected to be that which gives the highest CV-r^2. Bootstrap r^2 (Bs-r^2) is the average squared correlation coefficient calculated during the validation procedure.[21] A Bs-r^2 is computed from the subset of variables used one at a time for the validation procedure. It can be used more than one time in computing the r^2 statistic. Table 1 depicts structures of OA agonists, their experimental K_i values, calculated pK_i values using Equation (1), and difference between observed and calculated pK_i values. Values of pK_i (log of the reciprocal of K_i) were used as OA agonist activity index.

Color Plate 1a shows OA agonist NC 2,6-$(CH_2CH_3)_2$ (**38**) with the highest activity and OA agonist AAT 1-morpholino$(CH_2)_3$ (**30**) with the lowest activity embedded in an MFA generated from the OA agonist data set. A rigid fit was performed to superimpose each structure so that it overlays the shape reference compound **38**. The field of the entire agonist data set is represented and only the structures of **38** and **30** are embedded within the contours. The blue surface represents a contour for those points that correspond to a given positive contribution of the CH3 probe to pK_i. The blue surface is embedded with the most active OA agonist (**38**) in a desirable position. Meanwhile, the red surface represents a contour for those points corresponding to a given negative contribution. The red surface is embedded with the least active OA agonist (**30**) sticking out of the blue surface and thus, is in an undesirable position. The terms *H*+/420, *CH3*/732, and *HO*-/419 especially distinguish blue surface from red surface with respect to their activity. Note here that the grid points 419, 420, and 732 map in the variable part of the blue surface but not red surface.

To quantitatively understand the dependence of biological activities on MFA parameters of OA antagonists, regression analysis was applied to representative compounds listed in Figure 2 and Table 2, leading to Equation (2).

$$pK_i = 5.16568 - 0.000896H+/458 - 0.012485H+/544 - 0.04476H+/557 + 0.027549H+/573 + 0.006305CH3/246 - 0.014785CH3/248 - 0.021752CH3/376 - 0.001191CH3/436 - 0.020752CH3/449 - 0.015359CH3/580 + 0.035902CH3/655 + 0.047363CH3/670 + 0.057109HO-/366 - 0.010716HO-/475 \quad (2)$$

$$n = 20, \quad r^2 = 0.771, \text{CV-}r^2 = 0.886, \quad \text{Bs-}r^2 = 0.991 \pm 0.002$$

The structures and experimental activities (pK_i) of OA antagonists, the predicted activities (pK_i) using their top model, and differences between observed and calculated pK_i values are shown in Table 2. Color Plate 1b shows the OA antagonist

Table 2. Regression analysis of structure-OA antagonist activities

Compound			pK_i		
No.	R	K_1[a] (nm)	Observed	Calculated[b]	Deviation
71	Amitriptyline	1 570 ± 330	5.80	5.75	0.05
72	Antazoline	118 ± 62	6.93	6.94	−0.01
73	Chlorpromazine	766 ± 54	6.12	6.16	−0.06
74	Cyproheptadine	844 ± 356	6.07	6.00	0.07
75	Demethylmianserin	55 ± 3	7.26	7.25	0.01
76	Desipramine	3 210 ± 610	5.49	5.45	0.04
77	Dihydroergotamine	272 ± 29.9	6.57	6.65	−0.08
78	Eresepine	474 ± 166	6.32	6.24	0.08
79	Gramine	1 840 ± 1 012	5.74	5.84	−0.10
80	Hydroxymianserin	1.68 ± 0.49	8.77	8.76	0.01
81	Imipramine	1 450 ± 333	5.84	5.86	−0.02
82	Isopropylarterenol	18 600 ± 4 840	4.77	4.73	0.04
83	Maroxepine	1.02 ± 0.18	8.99	9.00	−0.01
84	Metoclopramide	52 601 ± 6 500	4.28	4.28	0
85	Mianserin	1.20 ± 0.27	8.92	8.93	−0.01
86	Phentolamine	19 ± 9	7.72	7.73	−0.01
87	Promethazine	32 ± 23	7.45	7.33	0.12
88	Propranolol	29 200 ± 11 920	4.53	4.59	−0.06
89	Triprolidine	2 900 ± 145	5.54	5.69	−0.15
90	Yohimbine	82 035 ± 22 400	4.09	4.01	0.08

[a] Cited from Roeder.[10]
[b] Calculated by Eq. (2).

maroxepine (**83**) with the highest activity and OA antagonist metoclopramide (**84**) with the lowest activity embedded in an MFA generated from an OA antagonist data set. A rigid fit was performed to superimpose each structure so that it overlays the shape reference compound **83**. The field of the entire antagonist data set is represented and only the structures of **83** and **84** are embedded within the contours. The blue surface represents a contour for those points that correspond to a given positive contribution of the CH3 probe to pK_i. The blue surface is embedded with the most active OA antagonist (**83**) in a desirable position. Meanwhile, the red surface represents a contour for those points corresponding to a given negative contribution. The red surface is embedded with the least active OA antagonist (**84**) sticking out of the blue surface and, thus, is in an undesirable position.

When agonists and antagonists were analyzed independently, correlation was unexpectedly good, leading to Eqs. (1) and (2), respectively. To quantitatively understand the dependence of biological activities on MFA parameters of OA agonists and antagonists together, regression analysis was applied to representative compounds listed in Figures 1 and 2, leading to Equation (3).

$$\begin{aligned} pK_i = {} & 4.53328 - 0.032172H+/558 + 0.039058H+/678 + \\ & 0.026163H+/776 - 0.023509H+/777 + 0.032808H+/ \\ & 788 - 0.039899H+/904 - 0.048928CH3/417 + \\ & 0.042704CH3/533 + 0.028557CH3/644 + 0.032911CH3/ \\ & 802 + 0.041016CH3/920 - 0.019139HO-/522 + \\ & 0.036603HO-/537 + 0.015175HO-/811 \quad (3) \end{aligned}$$

$n = 90$, $r^2 = 0.771$, CV-$r^2 = 0.626$, Bs-$r^2 = 0.755 \pm 0.002$

When agonists and antagonists were analyzed together, correlation was drastically decreased, leading to Eq. (3), compared with Eqs. (1) and (2), where agonists and antagonists were analyzed separately.

CONCLUSION

In drug discovery, it is common to have measured activity data for a set of compounds acting on a particular protein but not to have knowledge of the three-dimensional structure of the protein active site. In the absence of such three-dimensional information, one can attempt to build a hypothetical model of the receptor site that can provide insight about receptor site characteristics. Such a model is known as an MFA, which provides compact and quantitative descriptors that capture three-dimensional information about a putative receptor site. These models are predictive as judged by the CV-r^2 statistic and sufficiently reliable to guide the medicinal chemist in the design of novel compounds. These descriptors were used for predictive QSAR models. This approach is effective for the analysis of data sets where activity information is available but the structure of the receptor site is unknown. MFA attempts to postulate and represent the essential features of a receptor site from the aligned common features of the molecules that bind to it.

A pharmacophore model postulates that there is an essential three-dimensional arrangement of functional groups that a molecule must possess to be recognized by the receptor. It collects chemical features distributed in 3D space that is intended to represent groups in a molecule that participates in important

binding interactions between ligands and their receptors. Hence, a pharmacophore model provides crucial information about how well the chemical features of a subject molecule overlap with the hypothesis model. It also informs the ability of molecules to adjust their conformations in order to fit a receptor with energetically reasonable conformations. Pharmacophore models tend to be geometrically underconstrained (while topologically overconstrained); this steric underconstraint leads to false positives, that is, compounds that are deemed active by the model but that are inactive when tested. They postulate a 3D arrangement of atoms recognizable by the active site in terms of the similarity of functional groups common to the set of binding molecules.

MFA is also quantitative and a pharmacophore is qualitative. MFAs differ from pharmacophore models in that the former tries to capture essential information about the receptor, while the latter only captures information about the commonality of compounds that bind. MFAs tend to be geometrically overconstrained (and topologically neutral) since, in the absence of steric variation in a region, they assume the tightest steric surface that fits all training compounds. MFAs do not contain atoms, but try to directly represent the essential features of an active site by assuming complementarity between the shape and properties of the receptor site and the set of binding compounds. The MFA application uses 3D surfaces that define the shape of the receptor site by enclosing the most active members (after appropriate alignment) of a series of compounds. The global minimum of the most active compound (**38**) in the study table (based on the value in the activity column) was made as the active conformer. When there is no information on the actual "active conformation" of the ligands, MFA does not really describe the receptor; it describes a self-consistent field around the molecules that can explain activity. It really is just one of possibly many self-consistent models that fit the biological activity data.

When agonists and antagonists were analyzed together, correlation was drastically decreased. On the other hand, correlation was unexpectedly good when agonists and antagonists were analyzed separately, suggesting that agonists and antagonists have different structural features. However, although antagonists may not interact with the same part of the membrane with which the agonists interact, the presence of some common structural elements, such as the phenyl ring, suggests the binding sites may have some features in common. The ionophore, one component of the cell membrane, may be activated when a ligand and receptor interact. Antagonists may act via the receptor or the ionophore, or by a combination of both. Taking the part of the membrane with which the agonist interacts as the true receptor, the antagonist may well interact with an area surrounding the receptor, including the ionophore.

OA is not likely to penetrate either the cuticle or the central nervous system of insects effectively, since it is fully ionized at physiological pH. Derivatization of the polar groups would be one possible solution to this problem in trying to develop potential pest control agents. The above-described MFA studies show that agonists and antagonists with certain substituents can be potential ligands to OA receptors. These derivatives could provide useful information in the characterization and differentiation of octopaminergic receptor types and subtypes. They may help to point the way toward developing extremely potent and relatively specific OA ligands, leading to potential insecticides, although further research on the comparison of the 3D QSAR from agonists and antagonists is necessary. To optimize the activities of these compounds as OA ligands, more detailed experiments are in progress.

ACKNOWLEDGMENTS

This work was supported in part by a Grant-in-Aid for Scientific Research from the Ministry of Education, Science, and Culture of Japan.

REFERENCES

1 Axelrod, J., and Saavedra, J.M. Octopamine. *Nature (London)* 1977, **265,** 501–504
2 Evans, P.D. In: *Reviews in Comparative Molecular Neurobiology* (S.R. Heller, ed.). Birkhäuser Verlag, Basel, 1993, pp. 287–296
3 Evans, P.D. In: *Reviews in Comprehensive Insect Physiology, Biochemistry, and Pharmacology* (G.A Kerkut and G. Gilbert, eds.), Vol. 11. Pergamon Press, Oxford, 1985, pp. 499–530
4 Nathanson, J.A. Phenyliminoimidazolidines. Characterization of a class of potent agonists of octopamine-sensitive adenylate cyclase and their use in understanding the pharmacology of octopamine receptors. *Mol. Pharmacol.* 1985, **28,** 254–268
5 Evans, P.D. Multiple receptor types for octopamine in the locust. *J. Physiol.* 1981, **318,** 99–122
6 Roeder, T., and Nathanson, J.A. Characterization of insect neuronal octopamine receptors (OA3 receptors). *Neurochem. Res.* 1993, **18,** 921–925
7 Roeder, T., and Gewecke, M. Octopamine receptors in locust nervous tissue. *Biochem. Pharm.* 1990, **39,** 1793–1797
8 Roeder, T. A new octopamine receptor class in locust nervous tissue, the octopamine 3 (OA3) receptor. *Life Sci.* 1992, **50,** 21–28
9 Roeder, T. Pharmacology of the octopamine receptor from locust central nervous tissue (OAR3). *Br. J. Pharmacol.* 1995, **114,** 210–216
10 Roeder, T. High-affinity antagonists of the locust neuronal octopamine receptor. *Eur. J. Pharmacol.* 1990, **191,** 221–224
11 Jennings, K.R., Kuhn, D.G., Kukel, C.F., Trotto, S.H., and Whiteney, W.K. A biorationally synthesized octopaminergic insecticide: 2-(4-Chloro-*o*-toluidino)-2-oxazoline. *Pestic. Biochem. Physiol.* 1988, **30,** 190–197
12 Hirashima, A., Yoshii, Y., and Eto, M. Action of 2-aryliminothiazolidines on octopamine-sensitive adenylate cyclase in the American cockroach nerve cord and on the two-spotted spider mite *Tetranycus urticae* Koch. *Pestic. Biochem. Physiol.*, 1992, **44,** 101–107
13 Ismail, S.M.M., Baines, R.A., Downer, R.G.H., and Dekeyser, M.A. Dihydrooxadiazines: Octopaminergic system as a potential site of insecticidal action. *Pestic. Sci.* 1996, **46,** 163–170
14 Hirashima, A., Shinkai, K., Pan, C., Kuwano, E., Taniguchi, E., and Eto, M. Quantitative structure–activity studies of octopaminergic ligands against *Locusta migratoria* and *Periplaneta americana. Pestic. Sci.* 1999, **55,** 119–128
15 Pan, C., Hirashima, A., Tomita, J., Kuwano, E., Tanigu-

chi, E., and Eto, M. Quantitative structure–activity relationship studies and molecular modelling of octopaminergic 2-(substituted benzylamino)-2-thiazolines and oxazolines against nervous system of *Periplaneta americana* L. *Internet J. Sci. Biol. Chem.* 1997, **1,** http://www.netsci-journal.com/97v1/97013/index.htm
16 Hirashima, A., Pan, C., Tomita, J., Kuwano, E., Taniguchi, E., and Eto, M. Quantitative structure–activity studies of octopaminergic agonists and antagonists against nervous system of *Locusta migratoria. Bioorg. Med. Chem.* 1998, **6,** 903–910
17 Pan, C., Hirashima, A., Kuwano, E., and Eto, M. Three-dimensional pharmacophore hypotheses for the locust neuronal octopamine receptor (OAR3). 1. Antagonists. *J. Mol. Model.* 1997, **3,** 455–463
18 Hirashima, A., Pan, C., Kuwano, E., Taniguchi, E., and Eto, M. Three-dimensional pharmacophore hypotheses for the locust neuronal octopamine receptor (OAR3). 2. Agonists. *Bioorg. Med. Chem.* 1999, **7,** 1437–1443
19 Holland, J. In: *Adaptation in Artificial and Natural Systems.* University of Michigan Press, 1975
20 Friedman, J. In: *Multivariate Adaptive Regression Splines*; Technical Report 102. Laboratory for Computational Statistics, Department of Statistics, Stanford University, Stanford, 1988 (revised 1990)
21 Molecular Simulations. *Cerius2 Tutorial*, version 3.5. Molecular Simulations, Inc., San Diego, CA. (http://www.msi.com/doc/cerius35/)
22 Hansch, C., and Leo, A. In: *Exploring QSAR: Fundamentals and Applications in Chemistry and Biochemisry*. American Chemical Society, Washington, D.C., 1995
23 Hansch, C., and Fujita, T. ρ-σ-π analysis. A method for the correlation of biological activity and chemical structure. *J. Am. Chem. Soc.* 1964, **86,** 1616–1626
24 Golender, V.E., and Vorpagel, E.R. In: *3D-QSAR in Drug Design: Theory, Methods, and Applications* (H. Kubinyi, ed.). ESCOM Science Publishers, Amsterdam, The Netherlands, 1993, p. 137

Akinori Hirashima, Takumi Nagata, Canping Pan, Eiichi Kuwano, Eiji Taniguchi, and Morifusa Eto

Three-dimensional molecular field analyses of octopaminergic agonists and antagonists for the locust neuronal octopamine receptor class 3

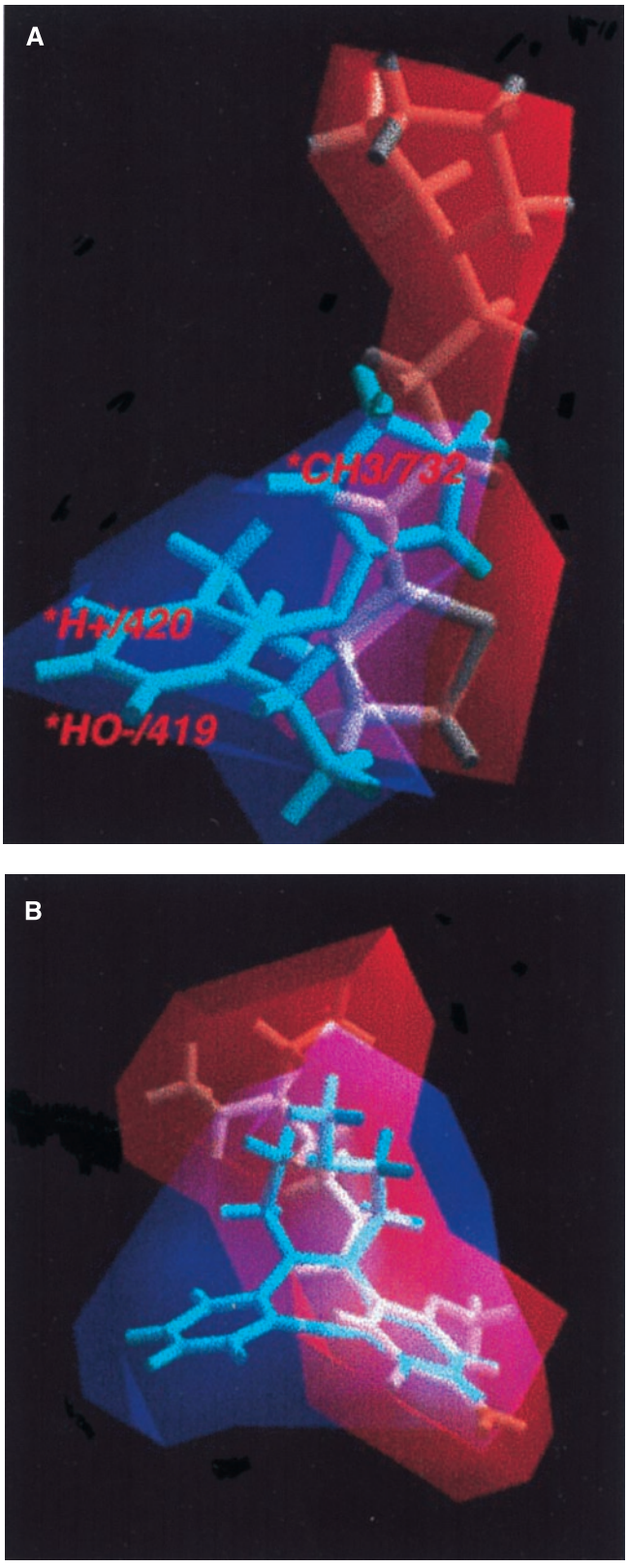

Color Plate 1. (a) The most active OA agonist (**38**) and the least active OA agonist (**30**) embedded in an MFA generated from OA agonist data set. The field of the entire agonist data set is represented and only the structures of **38** and **30** are embedded within the contours. The blue surface represents a contour for those points that correspond to a given positive contribution of the CH3 probe to pK_i. The blue surface is embedded with the most active OA agonist **38** in a desirable position. Note here that the grid points 419, 420, and 732 map in the variable part of the blue surface. The red surface represents a contour for those points corresponding to a given negative contribution. The red surface is embedded with the least active OA agonist **30** sticking out of the blue surface and thus, is in an undesirable position. (b) The OA antagonist with the highest activity (**83**) and the OA antagonist with lowest activity (**84**) embedded in an MFA generated from the OA antagonist data set. The field of the entire antagonist data set is represented and only the structures of **83** and **84** are embedded within the contours. The blue surface represents a contour for those points that correspond to a given positive contribution of the CH3 probe to pK_i. The blue surface is embedded with the most active OA antagonist (**83**) in a desirable position. The red surface represents a contour for those points corresponding to a given negative contribution. The red surface is embedded with the least active OA antagonist (**84**) protruding from the blue surface and, thus, is in an undesirable position.